

Oxidation of an *o*-Iminobenzosemiquinone Radical Ligand by Molecular Bromine: Structural, Spectroscopic, and Reactivity Studies of a Copper(II) *o*-Iminobenzoquinone Complex

Chandan Mukherjee, Thomas Weyhermüller, Eberhard Bothe, and Phalguni Chaudhuri*

Max-Planck-Institute for Bioinorganic Chemistry, Stiftstraße 34–36,
D-45470 Mülheim an der Ruhr, Germany

Received November 16, 2007

The bis(*o*-iminobenzosemiquinonato)copper(II) complex **1**, containing the radical form $[L^{\bullet}_{SQ}]^{1-}$ arising from the aerial oxidation of the noninnocent ligand 2-anilino-4,6-di-*tert*-butylphenol, H_2L , is readily oxidized by molecular bromine to a bis(*o*-iminobenzoquinone)copper(II) complex, **2**. Thus, a ligand-based oxidative addition is reported for complex **1** containing an electron-rich Cu^{II} d^9 metal ion. The crystal structure of the synthesized hexacoordinated complex $[Cu^{II}(L_{BQ})_2Br_2]$ (**2**) has been determined by X-ray crystallography at 100 K. Variable-temperature (2–290 K) magnetic susceptibility measurements and an X-band electron paramagnetic resonance spectrum establish the spin state to be $S_i = 1/2$ because of localized spin moments mainly in the $(d_{x^2-y^2})^1$ orbital of a Cu^{II} d^9 ion, indicating clearly the presence of a neutral iminobenzoquinone form, $[L_{BQ}]^0$, of the ligand in **2**, as is found also in the X-ray structure. Electrochemical measurements (cyclic voltammograms and coulometry) indicate two successive one-electron reductions of the ligand. The reactivity of complex **2** as an oxidizing agent toward ethanol and triethylamine has been investigated.

Introduction

This work stems from our interest in redox-active ligands, based on 2-aminophenol, which can coordinate to a metal ion not only in their deprotonated forms but also in their one-electron-oxidized *o*-iminobenzosemiquinone (SQ) radical and two-electron-oxidized *o*-iminobenzoquinone (BQ) closed-shell forms (Scheme 1).¹ Thus, we have described bis(*o*-iminobenzosemiquinonato)copper(II), $[Cu^{II}(L^{\bullet}_{SQ})_2]$ (**1**), which exhibits in electrochemistry four reversible one-electron redox processes, two oxidations, and two reductions;² all redox processes are shown to be ligand-based. Because metal

and quinone electronic levels are, in general, comparable in energy, facile metal–quinone electron transfer associated with valence tautomerism is observed and reported.³ Similar studies on charge distribution, from Cu^I (cat) species to the formation of Cu^I (SQ) redox isomers of copper with a change in the metal ion configuration from d^9 to d^{10} , are not well-known;^{3,5d} in most of the cases, the Cu^{II} state is reduced to Cu^I to be preferably bound to the benzoquinone (BQ) redox form of the ligand. Although the metal–benzoquinone (BQ) redox state has been established in the solid state for different transition-metal ions,^{3,4} examples of Cu^{II} BQ are very rare,⁵ and hence we have sought to find well-defined quinone complexes of Cu^{II} , inspired by quinoproteins⁶ that

* To whom correspondence should be addressed. E-mail: Chaudh@mpi-muelheim.mpg.de.

(1) (a) For example, see: Verani, C. N.; Gallert, S.; Bill, E.; Weyhermüller, T.; Wieghardt, K.; Chaudhuri, P. *Chem. Commun.* **1999**, 1747. (b) Chun, H.; Chaudhuri, P.; Weyhermüller, T.; Wieghardt, K. *Inorg. Chem.* **2002**, *41*, 790. (c) Mukherjee, S.; Weyhermüller, T.; Wieghardt, K.; Chaudhuri, P. *Dalton Trans.* **2003**, 3483. (d) Mukherjee, S.; Weyhermüller, T.; Bothe, E.; Wieghardt, K.; Chaudhuri, P. *Dalton Trans.* **2004**, 3842. (e) Kokatam, S.; Weyhermüller, T.; Bothe, E.; Chaudhuri, P.; Wieghardt, K. *Inorg. Chem.* **2005**, *44*, 3709. (f) Mukherjee, S.; Weyhermüller, T.; Bill, E.; Wieghardt, K.; Chaudhuri, P. *Inorg. Chem.* **2005**, *44*, 7099. (g) Mukherjee, C.; Weyhermüller, T.; Bothe, E.; Chaudhuri, P. *C. R. Chim.* **2007**, *10*, 313. (h) Mukherjee, C.; Weyhermüller, T.; Bothe, E.; Rentschler, E.; Chaudhuri, P. *Inorg. Chem.* **2007**, *46*, 9895, and references cited therein.

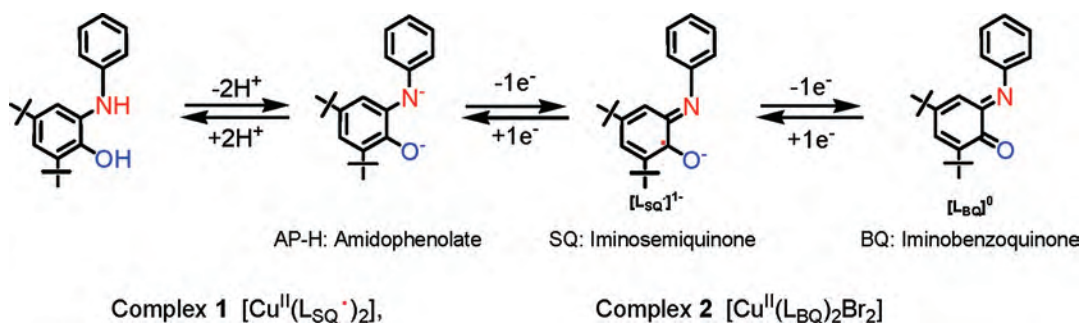
(2) Chaudhuri, P.; Verani, C. N.; Bill, E.; Bothe, E.; Weyhermüller, T.; Wieghardt, K. *J. Am. Chem. Soc.* **2001**, *123*, 2213.

(3) (a) Pierpont, C. G.; Lange, C. W. *Prog. Inorg. Chem.* **1994**, *41*, 331. (b) Pierpont, C. G. *Coord. Chem. Rev.* **2001**, *216–217*, 95.

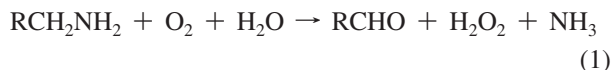
(4) Min, K. S.; Weyhermüller, T.; Wieghardt, K. *Dalton Trans.* **2003**, 1126, and references cited therein.

(5) (a) Salunke-Gawali, S.; Rane, S. Y.; Puranik, V. G.; Guyard-Duhaon, C.; Varret, F. *Polyhedron* **2004**, *23*, 2541. (b) Speier, G.; Tyeklár, Z.; Tóth, P.; Speier, E.; Tisza, S.; Rockenbauer, A.; Whalen, A. M.; Alkire, N.; Pierpont, C. G. *Inorg. Chem.* **2001**, *40*, 5643. (c) Castellani, C. B.; Gatti, G.; Millini, R. *Inorg. Chem.* **1984**, *23*, 4004. (d) Speier, G.; Csihony, J.; Whalen, A. M.; Pierpont, C. G. *Inorg. Chim. Acta* **1996**, *245*, 1.

Scheme 1



contain quinones as their cofactors. Copper amine oxidases (CAOs)⁶ are a class of such ubiquitous enzymes that catalyze the oxidation of amines to aldehydes:



CAOs belong to the class of “type 2” or “nonblue” copper proteins⁷ that utilize topaquinone 2,4,5-trihydroxyphenylalanine quinone as a redox cofactor to achieve deamination via an aminotransferase mechanism. While it is generally accepted that Cu^{II} does not play a redox role in the reductive half-reaction, the precise role of Cu^{II} in the oxidative half-reaction still remains controversial. A related enzyme, lysine oxidase,⁸ uses the similar cofactor lysine tyrosylquinone, which contains a cross-link between an ϵ -amino side chain of a lysine and a modified tyrosine within the same polypeptide chain.

The above bioinspiring motif has prompted us to explore the selective transformation of *o*-iminobenzosemiquinone, L_{SQ} (Scheme 1), via the transfer of electrons promoted by redox agents. In this report, we describe observations on the oxidation of **1** by molecular bromine. We report here the synthesis of a hexacoordinated Cu^{II} complex with Cu^{II} –BQ bonds, complex **2**, along with its spectroscopic, electrochemical, structural characterization, and reactivity studies.

Experimental Section

Materials and Physical Measurements. Reagent-grade chemicals were used in all experiments, and solvents were purified by standard procedures. Fourier transform (FT)-IR spectra of the samples in KBr disks were recorded with a Perkin-Elmer 2000 FT-

IR instrument. Electronic absorption spectra in solution were measured with a Perkin-Elmer Lambda 19 spectrophotometer. Spectra of the spectroelectrochemical investigations were recorded on an HP 8452A diode array spectrophotometer (range: 221–1100 nm). Cyclic voltammograms, square-wave voltammograms, and coulometric experiments were performed using an EG&G potentiostat/galvanostat (model 273A). Mass spectra were recorded with either a Finnigan MAT8200 (electron ionization, EIMS) or a MAT95 (electrospray, ESI-MS) instrument. Magnetic susceptibilities were recorded with a SQUID magnetometer (MPMS Quantum Design) in the temperature range 2–290 K with an applied magnetic field of 1.0 T. The experimental susceptibility data were corrected for underlying diamagnetism by the use of tabulated Pascal’s constants. X-band electron paramagnetic resonance (EPR) spectra were recorded with a Bruker ELEXSYS E500 spectrometer equipped with a helium-flow cryostat (Oxford Instruments ESR 910).

Preparations. The ligand 2-anilino-4,6-di-*tert*-butylphenol, H_2L , and complex **1**, $[\text{Cu}^{\text{II}}(\text{L}_{\text{SQ}})_2]$, were prepared using procedures described previously.²

Preparation of $[\text{Cu}^{\text{II}}(\text{L}_{\text{BQ}})_2\text{Br}_2]$ (2**).** To a dark-green solution of complex **1** (0.65 g, 1 mmol) in degassed dichloromethane (30 mL) was added bromine (50 μL , 1 mmol) under an argon atmosphere. The resulting dark-brown solution was stirred for 1 h, followed by the addition of 10 mL of *n*-hexane; a slow stream of argon was passed through to concentrate the solution. Precipitated deep-brown crystals of **2** were isolated by filtration and washed with *n*-hexane. Yield: 0.43 g (52%). IR (KBr, cm^{-1}): 2967–2867s, 1647s, 1621s, 1533m, 1482s, 1451m, 1396m, 1380s, 1368s, 1308m, 1271m, 1253m, 1209m, 1073m, 1027m, 977m, 900s, 796m, 804m, 763s, 737s, 699s. ESI-MS (CH_2Cl_2): m/z 813 $[\text{M}]^+$, 733 $[\text{M} - \text{Br}]^+$, 653 $[\text{M} - 2\text{Br}]^+$. UV–vis (CH_2Cl_2 ; λ , nm (ϵ , $\text{M}^{-1} \text{cm}^{-1}$): 310 (1.116×10^4), 430 (9600), 675sh (~ 410). Anal. Calcd for $\text{C}_{40}\text{H}_{50}\text{N}_2\text{O}_2\text{Br}_2\text{Cu}$: C, 59.00; H, 6.19; N, 3.44; Br, 19.63; Cu, 7.81. Found: C, 59.2; H, 6.1; N, 3.3; Br, 19.7; Cu, 7.7.

X-ray Crystallographic Data Collection and Refinement of the Structure. A single crystal of **2** was coated with perfluoropolyether, picked up with glass fibers, and mounted on a Nonius Kappa CCD diffractometer equipped with a cryogenic nitrogen cold stream operating at 100(2). Graphite-monochromated Mo $\text{K}\alpha$ radiation ($\lambda = 0.71073 \text{ \AA}$) was used. Intensity data were corrected for Lorentz and polarization effects. No absorption correction was carried out. The Siemens *SHELXTL* software package⁹ (G. M. Sheldrick, Universität Göttingen, Göttingen, Germany) was used for solution, refinement, and artwork of the structure, and neutral atom scattering factors of the program were used. The structure was solved and refined by direct methods and difference Fourier techniques. Non-

(6) (a) For example, see: Dooley, D. M. *J. Biol. Inorg. Chem.* **1994**, *4*, 1. (b) Klinman, J. P.; Mu, D. *Annu. Rev. Biochem.* **1994**, *63*, 299. (c) Dove, J. E.; Klinman, J. P. *Adv. Protein Chem.* **2001**, *58*, 141. (d) Klinman, J. P. *J. Biol. Chem.* **1996**, *271*, 27189. (e) Parsons, M. R.; Convery, M. A.; Wilmot, C. M.; Yadav, K. D. S.; Blakeley, V.; Comer, A. S.; Philips, A. E. V.; McPherson, M. J.; Knowles, P. F. *Structure* **1995**, *3*, 1171. (f) Kumar, V.; Dooley, D. M.; Freeman, H. C.; Guss, J. M.; Harvey, I.; McGuirl, M. A.; Wilce, M. C. J.; Zubak, V. M. *Structure* **1996**, *4*, 943. (g) Li, R.; Klinman, J. P.; Mathews, F. S. *Structure* **1998**, *6*, 293. (h) Mure, M.; Mills, S. A.; Klinman, J. P. *Biochemistry* **2002**, *41*, 9269. (i) Mure, M. *Acc. Chem. Res.* **2004**, *37*, 131, and references cited therein. (j) Dubois, J. L.; Klinman, J. P. *Biochemistry* **2006**, *45*, 3178, and references cited therein.

(7) *Multicopper Oxidases*; Messerschmidt, A., Ed.; World Scientific: Singapore, 1997.

(8) Wang, S. X.; Mure, M.; Medzihradsky, K. F.; Buclingame, A. L.; Brown, D. E.; Dooley, D. M.; Smith, A. J.; Kagan, H. M.; Klinman, J. P. *Science* **1996**, *273*, 1078.

(9) (a) *SHELXTL*, version 5; Siemens Analytical X-ray Instruments, Inc.: Madison, WI, 1994. (b) Sheldrick, G. M. *SHELXL97*; Universität Göttingen: Göttingen, Germany, 1997.

Table 1. Crystallographic Data for Complex **2**·CH₂Cl₂

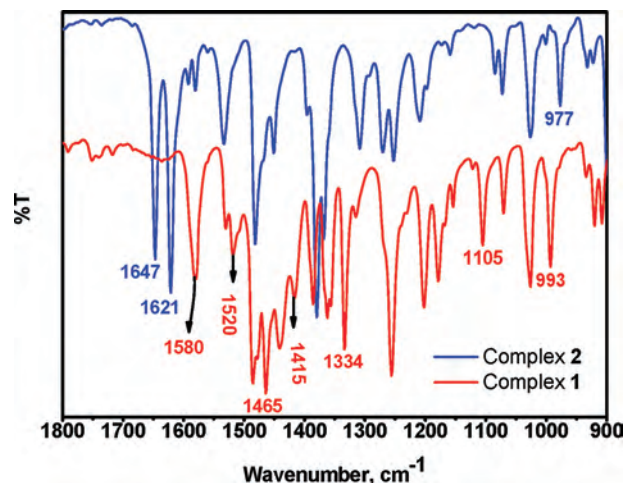
empirical formula	C ₄₁ H ₅₂ Br ₂ Cl ₂ CuN ₂ O ₂
fw	899.11
temperature (K)	100(2)
λ (Mo K α) (Å)	0.710 73
cryst syst	monoclinic
space group	<i>P</i> 2(1)/ <i>c</i>
unit cell dimens	<i>a</i> = 9.6530(3) Å, <i>b</i> = 20.1784(6) Å, <i>c</i> = 11.4904(4) Å, α = 90°, β = 100.675(4)°, γ = 90°
volume (Å ³), <i>Z</i>	2199.39(12), 2
ρ (calcd) (Mg/m ³)	1.358
abs coeff (mm ⁻¹)	2.468
<i>F</i> (000)	922
cryst size (mm)	0.07 × 0.07 × 0.03
θ range for data collcn, deg	3.21–30.00
reflns collected/unique	34942/6405 [<i>R</i> (int) = 0.0642]
completeness to θ = 30°	99.8 (%)
refinement method	full-matrix least squares of <i>F</i> ²
data/restraints/param	6405/6/257
GOF on <i>F</i> ²	1.064
final <i>R</i> indices [<i>I</i> > 2 σ (<i>I</i>)]	<i>R</i> 1 = 0.0453, w <i>R</i> 2 = 0.0972
<i>R</i> indices (all data)	<i>R</i> 1 = 0.0675, w <i>R</i> 2 = 0.1081

hydrogen atoms were refined anisotropically, and hydrogen atoms were placed at calculated positions and refined as riding atoms with isotropic displacement parameters. A CH₂Cl₂ molecule next to a crystallographic inversion center was found to be disordered. The molecule was split at two positions (~80:20), C–Cl and Cl⋯Cl distances of the split components were restrained to be equal within errors, and equal anisotropic displacement parameters were used. Details of data collection and structure refinements are summarized in Table 1.

Results and Discussion

Complex **1** is readily available in a good yield from the reaction of H₂L and CuCl (ratio 2:1) in CH₃CN in the presence of air, as was described earlier.² We presented structural and spectroscopic evidence for the formulation of **1** as a diradical with a Cu^{II} d⁹ ion. Facile generation of the radical form of the ligand [L[•]_{SQ}][−] presumably occurs through oxidation by aerial oxygen, indicating also the nonavailability of the two-electron-oxidized quinone form [L_{BQ}]⁰ of the ligand via aerial oxidation (Scheme 1). To attain the oxidation potential of $E_{1/2}^{\text{ox}} = 0.37$ V vs Fc⁺/Fc, as determined from the electrochemical measurements of **1**, for generation of the quinone form of the ligand, we have chosen molecular bromine as an oxidizing agent because the reduction potential of bromine, a one-electron oxidizing agent, is higher than the two-electron reduction potential of dioxygen. To our satisfaction, the desired product, complex **2**, with the Cu^{II}–L_{BQ} bonds was readily isolated as a deep-brown crystalline solid.

A tetracoordinated square-planar complex, **1**, is easily oxidized to complex **2** with an increase in the coordination number to 6 by bromide addition. Each of the radical ligands in **1** is oxidized by one electron to the quinone form present in **2**, thus providing the necessary redox equivalents. Formally the metal center has not taken part in the redox process and remains unchanged in its physical (spectroscopic) oxidation state, Cu^{II}. Thus, a complex of Cu^{II}, an electron-rich metal ion without readily accessible M^{*n*+} and M^{*(n+2)+*} oxidation states, exhibits oxidative addition reactivity. Recently, similar ligand-based oxidative addition

**Figure 1.** Selected IR spectra of complexes **1** and **2**.

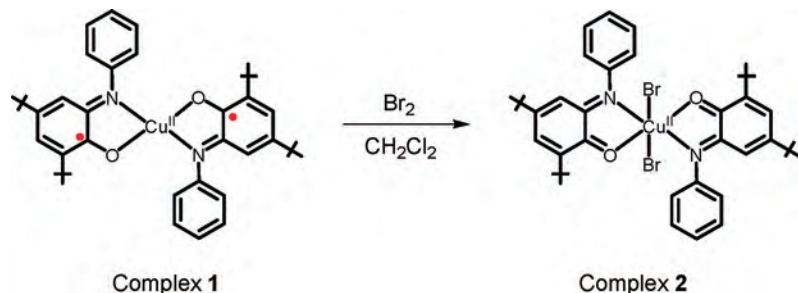
has been reported for a Zr^{IV} complex,¹⁰ in which each of the two amidophenolate ligands were converted to their radical semiquinone forms via one-electron oxidation (Scheme 1).

The IR spectrum of complex **2** differs markedly as expected from that of complex **1**, which contains the radical iminosemiquinone form of the ligand, whereas the iminobenzoquinone form is present in complex **2**. For comparison purposes, the IR spectra (1800–900 cm^{−1}) are shown in Figure 1. The strong bands at 1580, 1520, 1465, 1415, 1334, and 1105 cm^{−1} attributable to $\nu(\text{C}\cdots\text{O})$, $\nu(\text{C}\cdots\text{N})$, and $\nu(\text{C}–\text{C})$ bond deformations in the *tert*-butyl-containing benzene ring of the ligand in complex **1** disappear upon oxidation with the concomitant appearance of two strong stretches at 1647 and 1621 cm^{−1} due to the $\nu(\text{C}=\text{O})$ and $\nu(\text{C}=\text{N})$ groups¹¹ present in complex **2**. This disparity in the number of IR bands is an indication of delocalization of the radical electron in the quinoid-distorted benzene ring in **1**, whereas **2** is devoid of this electron. Similar IR bands have been reported earlier for other transition-metal complexes. The band at 993 cm^{−1} in complex **1**, attributable to the $\nu[\text{Cu}–\text{O}(\text{phenoxide})]$ stretch, shifts to 973 cm^{−1} for complex **2** after oxidation.

The structure of complex **2** consists of neutral, centrosymmetric mononuclear molecule [Cu^{II}(L_{BQ})₂Br₂], which contains one molecule of CH₂Cl₂ as a solvent of crystallization. Selected bond lengths and angles are given in Table 2. An ORTEP view of the neutral molecule is shown in Figure 2. The asymmetric unit contains half of the molecule, and consequently the metrical parameters of two chelating ligands are identical, with ligation provided by two oxygen and two nitrogen atoms belonging to two ligands and two bromide ions in the trans positions of an octahedron. The overall geometry around the copper Cu(1) ion is best described as a distorted octahedron with two cis-positioned oxygen O(1) and N(8) belonging to the aminophenol-based ligand, whereas Br(1) occupies the remaining coordination site of

(10) Blackmore, K. J.; Ziller, J. W.; Heyduk, A. F. *Inorg. Chem.* **2005**, *44*, 5559.

(11) *Infrared Spectra of Inorganic and Coordination Compounds*; Nakamoto, K. Wiley-Interscience: New York, 1970.

**Table 2.** Selected Bond Angles (deg) and Bond Distances (Å) for Complex **2**

Br(1)–Cu(1)	2.4676(3)	C(9)–C(10)	1.384(4)
Cu(1)–N(8)	1.992(2)	C(9)–C(14)	1.391(4)
Cu(1)–O(1)	2.3803(19)	C(10)–C(11)	1.392(4)
O(1)–C(2)	1.223(3)	C(11)–C(12)	1.380(4)
C(2)–C(3)	1.477(3)	C(12)–C(13)	1.381(5)
C(2)–C(7)	1.523(4)	C(13)–C(14)	1.390(4)
C(3)–C(4)	1.359(4)	N(8)–Cu(1)–N(8A)	180.00
C(4)–C(5)	1.468(4)	N(8)–Cu(1)–O(1A)	104.94(8)
C(5)–C(6)	1.351(4)	N(8)–Cu(1)–O(1)	75.06(8)
C(6)–C(7)	1.440(4)	O(1)–Cu(1)–O(1A)	180.00
C(7)–N(8)	1.298(3)	Br(1)–Cu(1)–Br(1A)	180.00
N(8)–C(9)	1.433(3)	C(7)–N(8)–C(9)	119.7(2)
		C(7)–N(8)–Cu(1)	120.99(18)
		C(9)–N(8)–Cu(1)	119.16(17)

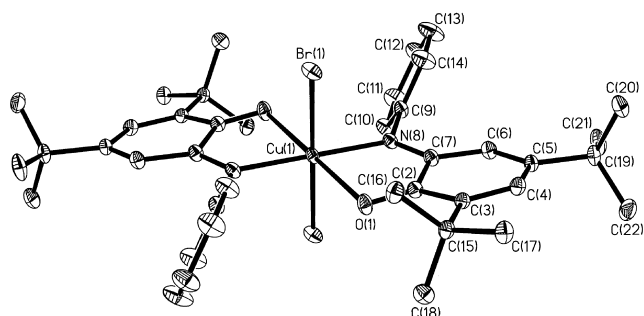
one face of an octahedron. The distortion from octahedral geometry is mainly caused by the bite angles involving the oxygen O(1) and nitrogen N(8) of the ligand. The O(1)–Cu(1)–N(8) and O(1)–Cu(1)–N(8*) angles are 75.06(8) and 104.93(8)°, respectively, while the Br(1)–Cu(1)–O(1) and Br(1)–Cu(1)–N(8) angles at 88.77(5) and 88.49(6)°, respectively, do not deviate far from the ideal 90°. The phenyl rings attached to the nitrogen atoms, N(8) and N(8*), are found as expected to be planar, indicating that the conjugation resulting in the aromaticity of the phenyl ring is retained. The C(2)–O(1) and C(7)–N(8) bonds of the aminophenol-derived ligands at 1.223(3) and 1.298(3) Å, respectively, are significantly shorter than the comparable bonds at 1.290(4) and 1.335(4) Å of **1**, indicating the higher level of oxidation of the ligand, i.e., the benzoquinone form, in complex **2**. In addition, a true quinone structure with two alternating C=C double bonds at 1.355(8) Å and four longer single bonds are observed for the phenyl ring with the *tert*-butyl substituents.

Furthermore, the Cu(1)–N(8) and Cu(1)–Br(1) bond lengths¹² at 1.992(2) and 2.468(1) Å, respectively, are typical for octahedral Cu^{II} ions (d⁹, $S_{\text{Cu}} = 1/2$), whereas the observed Cu(1)–O(1) distance at 2.380(2) Å is remarkably longer than

that in complex **1** with the semiquinone ligand at 1.912(2) Å,² thus leading to the unambiguous assignment of the oxidation level of the ligand to be the neutral iminobenzoquinone form. However, it is noteworthy that Cu–N and Cu–O bond lengths in Cu₂(PhenBQ)₂(μ-Cl)₂,^{5d} where PhenBQ represents 2,4,6,8-tetra-*tert*-butylphenoxazin-1-one, are comparable with those for **2**. Thus, neutral complex **2** is composed of two bromide anions, two iminobenzoquinone ligands, and one hexacoordinated Cu^{II} ion, which is present in the equatorial plane comprised of N(8), N(8*), Br(1), and Br(1*) atoms, and the axial positions are occupied by O(1) and O(1*) atoms. Complex **2** is a rare example of a structurally characterized mononuclear Cu^{II} coordination compound with two O,N-coordinated *o*-iminobenzoquinone ligands. A chain-structured Cu^{II} complex containing the 2-hydroxy-1,4-naphthoquinone ligand exhibits very similar, like that of **2**, Cu^{II}–quinone bond lengths.^{5a}

That complex **2** contains the diamagnetic, O,N-coordinated *o*-iminobenzoquinone ligand coordinated to a Cu^{II} center has also been established by variable-temperature (2–290 K) magnetic susceptibility measurements on a powdered sample of **2** using a SQUID magnetometer. Complex **2** exhibits above 10 K essentially temperature-independent magnetic moment values $\mu_{\text{eff}} = 1.77 \pm 0.01 \mu_{\text{B}}$ (Figure S1 in the Supporting Information) and thus contains clearly an $S = 1/2$ spin state. A good fit of the experimental data, shown as a solid line in Figure S1 (Supporting Information), is obtained using the fit parameters $S_{\text{t}} = 1/2$, $g = 2.051$, and θ (Weiss constant) = –0.13 K. That the paramagnetism with $S = 1/2$ originates from the Cu^{II} center (d⁹) and not from the radical semiquinone form of the ligand is reflected in the fitted g value of 2.051, which is further substantiated by the X-band EPR spectrum of **2**.

Because Cu^{II} (d⁹) ions exhibit significant g anisotropy and large hyperfine splittings contrasting in this respect to the coordinated organic radical anions,^{13–16} it is possible to probe the origin of the ground state by X-band EPR spectroscopy. Figure 3 shows the experimental X-band EPR spectrum of complex **2** in CH₂Cl₂ at 30 K, together with its simulation. The EPR spectrum exhibits axial g values with slight rhombic distortions and ^{63/65}Cu hyperfine

**Figure 2.** Molecular structure of complex **2**.

(12) Shvedenkov, Y.; Bushuev, M.; Romanenko, G.; Lavrenova, L.; Ikorskii, V.; Gaponik, P.; Larionov, S. *Eur. J. Inorg. Chem.* **2005**, 1678.

(13) Kaim, W. *Coord. Chem. Rev.* **2001**, 219–221, 463.

(14) Gatteschi, D.; Bencini, A. *Electron Paramagnetic Resonance of Exchange Coupled Systems*; Springer-Verlag: New York, 1990.

(15) DeBolfo, J. A.; Smith, T. D.; Boas, J. F.; Pilbrow, J. R. *Aust. J. Chem.* **1976**, 29, 2583.

(16) Hathaway, B. J.; Billing, D. E. *Coord. Chem. Rev.* **1970**, 5, 143.

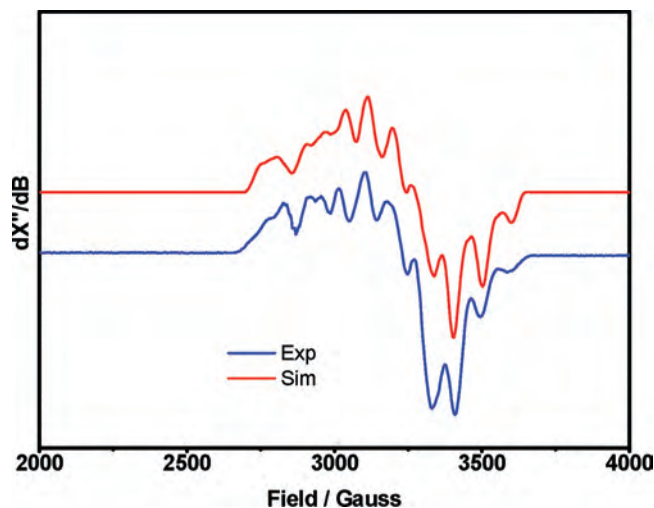


Figure 3. X-band EPR spectrum of **2** at 30 K in CH_2Cl_2 . $g_1 = 2.02, 2.085, 2.205$; $A^{\text{Cu}} = (24, 3, 138) \times 10^{-4} \text{ cm}^{-1}$.

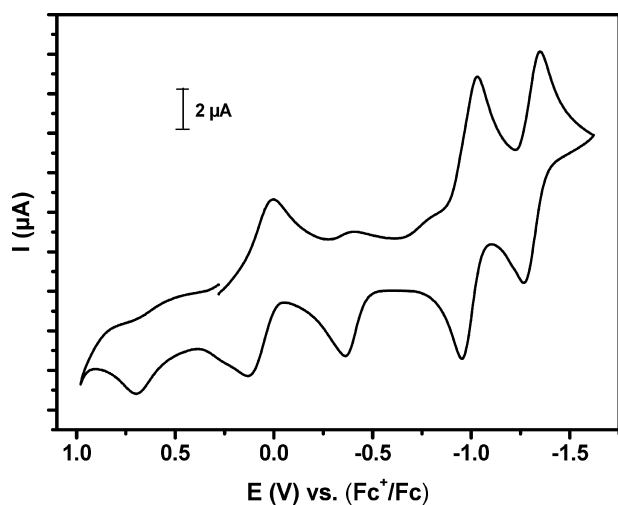


Figure 4. Cyclic voltammogram of $1 \times 10^{-3} \text{ M}$ complex **2** recorded in a CH_2Cl_2 solution containing 0.2 M $[\text{N}(\text{n-Bu})_4]\text{PF}_6$ as the supporting electrolyte at a scan rate of 100 mV s^{-1} at $+25^\circ \text{C}$. (Conditions: glassy carbon working electrode.)

splittings (Figure 3) close to values expected for single-ion Cu^{II} complexes with a $(d_{x^2-y^2})^1$ magnetic orbital. Interestingly, the spectrum shows a distinct ligand hyperfine splitting, and a satisfactory simulation was obtained with two equivalent ^{14}N nuclei ($I = 1$) with $A_{\text{N}} = (90, 90, 30) \times 10^{-4} \text{ cm}^{-1}$. This anisotropy is presumably due to spin-dipolar contributions of S_{Cu} with spin density in the $d_{x^2-y^2}$ orbital. Thus, the magnetic results for **2** do demonstrate the presence of a central Cu^{II} ion coordinated to a diamagnetic closed-shell ligand.

Electro- and Spectroelectrochemistry. Cyclic voltammograms of complex **2** have been recorded in CH_2Cl_2 solutions containing 0.2 M $[\text{N}(\text{n-Bu})_4]\text{PF}_6$ as the supporting electrolyte at a glassy carbon working electrode and a Ag/AgNO_3 reference electrode. Ferrocene was used as an internal standard, and all potentials are referenced versus the ferrocene couple Fc^+/Fc .

Figure 4 shows a cyclic voltammogram of **2**. The potential at which no current flows when the voltage is applied is around $+0.2 \text{ V}$. During cathodic scans, starting from $+0.2$

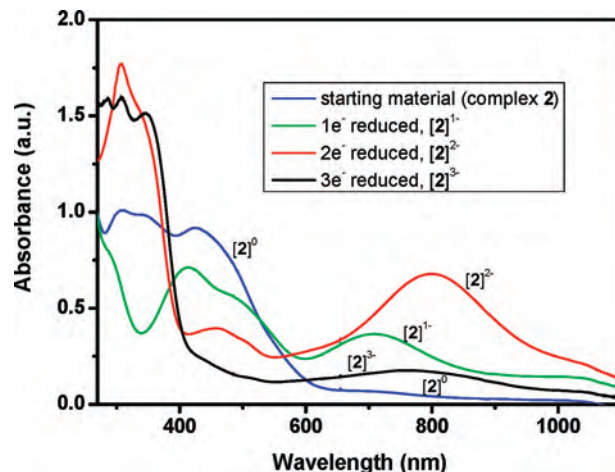
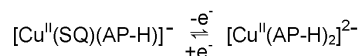
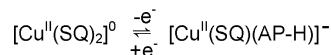
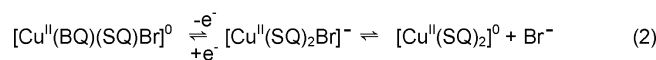
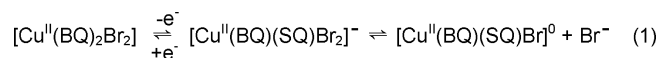


Figure 5. Electronic spectra (at -25°C) of electrochemically generated reduced forms of **2** after one-, two-, and three-electron reductions in CH_2Cl_2 solutions containing 0.2 M $[\text{N}(\text{n-Bu})_4]\text{PF}_6$.

Scheme 2



V, successive reduction waves became discernible, but only the two at the most negative potentials showed the feature characteristic for a reversible one-electron-transfer wave: reduction and reoxidation peaks of equal height are separated by about 80 mV , a typical value for reversible electron transfer in this solvent. The formal reduction potentials for these reductions are -1.01 and -1.32 V . Both values fully coincide with those of the analogous compound *without* axial Br^- ligands, i.e., complex **1**. This suggests that the more complex reductive processes preceding the two reversible reductions at more positive potentials must be accompanied by the loss of both Br^- ligands.

Electronic spectra recorded during controlled potential coulometric reductions (at -25°C) showed indeed that after passage of two electrons per molecule the spectrum of the neutral, Br^- -free $[\text{Cu}(\text{L}^{\cdot}\text{SQ})_2]^0$ species appeared (see Figure 5). After passage of three electrons, the spectrum of the Br^- -free monoanion $[\text{Cu}^{\text{II}}(\text{SQ})(\text{AP-H})]^-$ developed. This leads to the reaction in Scheme 2 and consequently the spectrum observed after one electron is assigned to the neutral complex $[\text{Cu}^{\text{II}}(\text{BQ})(\text{SQ})\text{Br}]^0$. The dianion $[\text{Cu}^{\text{II}}(\text{AP-H})_2]^{2-}$ could not be generated electrochemically, possibly because of its limited stability under our conditions.

It is noted that throughout the coulometric experiments, the cyclic voltammograms observed remained almost unchanged, demonstrating the chemical reversibility of the system of eq 1 in Scheme 2. This is corroborated by the finding that under no conditions free Br^- was detected in the cyclic voltammograms, which would have given rise to

Acknowledgment. This work is supported by the Max-Planck Society and the German Research Council (Deutsche Forschungsgemeinschaft) (Project: Priority Program “Radicals in Enzymatic Catalysis”). Skillful technical assistance of H. Schucht, U. Westhoff, A. Göbels, and F. Reikowski is thankfully acknowledged.

Supporting Information Available: X-ray crystallographic data in CIF format and plot of $\mu_{\text{eff}}/\mu_{\text{B}}$ vs T/K for complex **2**. This material is available free of charge via the Internet at <http://pubs.acs.org>.

IC702256P